

NMR on Anisotropic Magnetic Moment of Surface Bound States in Topological Superfluid $^3\text{He-B}$

M. Človečko, E. Gažo, M. Skyba, and P. Skyba*

Centre of Low Temperature Physics, Institute of Experimental Physics SAS, Watsonova 47, 04001 Košice, Slovakia.

(Dated: January 8, 2019)

We present experimental observation of a new NMR effect on anisotropic magnetic moment of the surface Andreev-Majorana bound states in topological superfluid $^3\text{He-B}$ in zero temperature limit. We show that an anisotropic magnetic moment formed near the horizontal surface of a mechanical resonator due to symmetry violation of the superfluid $^3\text{He-B}$ order parameter by the resonator's surface may lead to anomalous damping of the resonator motion in magnetic field. In difference to classical NMR technique, here NMR was excited using own harmonic motion of the mechanical resonator, and nuclear magnetic resonance was detected as a maximum in damping when resonator's angular frequency satisfied the Larmor resonance condition.

PACS numbers: 67.30.-n, 67.30.H-, 67.30.hj, 67.30.er, 67.80.D-, 67.80.dk

INTRODUCTION

Superfluid phases of helium-3 provide one of the most complex and purest physical system to which we have access to. This unique system is also serving as a model system for high energy physics, cosmology and quantum field theories. In fact, the phase transition of ^3He into a superfluid state violates simultaneously three symmetries: the orbital, the spin and the gauge symmetry ($\text{SO}^L(3) \times \text{SO}^S(3) \times \text{U}(1)$). Either A or B superfluid phase of ^3He created in zero magnetic field resembles the physical features comparable with those described by the Standard model or by the Dirac vacuum, respectively [1]. Application of magnetic field breaks the spin symmetry and this leads to formation of A_1 phase in narrow region just below superfluid transition temperature [2]. Further, embedding of the anisotropic impurity into ^3He in form e.g. nematically ordered aerogel violates the orbital symmetry, which is manifested by formation of a polar phase of superfluid ^3He [3, 4]. Finally, the orbital symmetry of the superfluid condensate is also violated near the surface of any object of the size of the coherence length ξ ($\xi \sim 100 \text{ nm}$) being immersed in superfluid $^3\text{He-B}$. Presence of the surface enforces only the superfluid component that consists of the Cooper pairs having their orbital momenta oriented in direction to the surface normal and suppresses all others. This results in the distortion of the energy gap in direction parallel to the surface normal on the distance of a few coherence lengths from the surface. The gap distortion leads to a strong anisotropy in spin susceptibility of the superfluid surface layer of ^3He [5], as well as to the motional anisotropy of fermionic excitations trapped in surface Andreev bound states (SABS). It is worth to note that the dispersion relation of some of these excitations resembles the features of Majorana fermions, the fermions, which are their own antiparticles [6–9].

This article deals with experimental observations of an effect of nuclear magnetic resonance (NMR) performed

on surface magnetic layer in superfluid $^3\text{He-B}$ at temperature of $175 \mu\text{K}$ and pressure of 0.1 bar. However, in contrast to traditional NMR techniques, the magnetic resonance was excited using a mechanical resonator oscillating in magnetic field and detected as an additional magnetic field dependent mechanical damping of the resonator's motion.

In order to be able to study physical properties of the surface states, the superfluid $^3\text{He-B}$ has to be cooled to zero temperature limit. When superfluid $^3\text{He-B}$ is cooled below $250 \mu\text{K}$, the quasiparticle flux of the volume excitations falls with temperature as $\phi_V \sim D(p_F)T \exp(-\Delta/k_B T)$ due to presence of the energy gap Δ in the spectrum of excitations [21]. Here, $D(p_F)$ denotes the density of states on the Fermi level, p_F is the Fermi momentum and k_B is the Boltzmann constant. On the other hand, the gap distortion in vicinity of the surface modifies the dispersion relation for the excitations trapped in SABS to "A-like" phase and corresponding flux of the surface excitations ϕ_S varies non-exponentially ($\phi_S \sim D_S(p_F)T^3$), where $D_S(p_F)$ is the density of states near surface which depends on the surface quality. Therefore, one may expect that in superfluid $^3\text{He-B}$ at higher temperatures $\phi_S < \phi_V$ (in a hydrodynamic regime), while at ultra low temperatures (in a ballistic regime) a state when $\phi_S > \phi_V$ can be achieved. This temperature transition can be detected using e. g. mechanical resonators as a decrease of their sensitivity to the collisions with volume excitations with temperature drop. It is obvious that this transition temperature depends on the resonator's mass, the area and quality of the resonator's surface which determines the density of the surface states [5, 10–12].

There are variety of mechanical resonators being used as experimental tools to probe the physics of topological $^3\text{He-B}$ at zero temperature limit [13–16]. As mechanical resonators we utilize tuning forks. Currently, these piezoelectric devices are very popular experimental tools used in superfluid ^3He physics [17]. They are almost magnetic

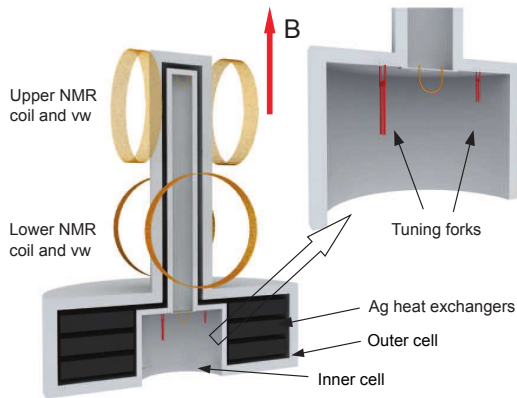


FIG. 1: (Color online) A schematic sketch of the double walled experimental cell mounted on our nuclear stage. The orientation of magnetic field B is shown as well.

field insensitive, simple to install, easy to excite with extremely low dissipation of the order of a few fW or even less and displacement $\sim 0.1\text{nm}$ and straight forward to measure. The measured current I_F is proportional to the fork velocity $I_F = Av$, where A is the proportionality constant readily determined from experiment [18, 19].

EXPERIMENTAL DETAILS

We performed experiments in a double walled experimental cell mounted on a diffusion-welded copper nuclear stage (see Fig. 1) [20]. While upper tower served for NMR measurements (not mentioned here), in the lower part of the experimental cell, tuning forks of different sizes and one NbTi vibrating wire were mounted. The NbTi vibrating wire served as a thermometer of $^3\text{He-B}$ in ballistic regime i.e. in temperature range below $250\mu\text{K}$.

After cooling the fridge down to $\sim 0.9\text{K}$, we initially characterized the tuning forks in vacuum using a standard frequency sweep technique in order to determine A constants for the individual forks [17, 18]. Both forks behaved as high Q-value resonators having Q-value of the order of 10^6 . The physical characteristics of the large and small tuning forks are as follow: the large fork resonance frequency (in vacuum) $f_0^L = 32725.88\text{Hz}$, the width $\Delta f_{2i} = 36.3\text{mHz}$ and dimensions $L = 3.12\text{mm}$, $W = 0.25\text{mm}$, $T = 0.402\text{mm}$ give the mass $m_L = 2.0 \times 10^{-7}\text{kg}$ and value of $A_L = 6.26 \times 10^{-6}\text{A.s.m}^{-1}$, while the small fork resonance frequency $f_0^S = 32712.968\text{Hz}$, the width $\Delta f_{2i} = 32.79\text{mHz}$ and dimensions $L = 1.625\text{mm}$, $W = 0.1\text{mm}$, $T = 0.1\text{mm}$ give the mass $m_S = 1.05 \times 10^{-8}\text{kg}$ and the value of $A_S = 1.04 \times 10^{-6}\text{A.s.m}^{-1}$.

Then, we filled the experimental cell with ^3He at pressure of 0.1 bar. Subsequent demagnetizations of the cop-

per nuclear stage allowed us to cool the superfluid $^3\text{He-B}$ in the inner cell down to $175\mu\text{K}$ as determined from the damping of the NbTi vibrating wire.

We also performed measurements of tuning forks in small magnetic fields. After demagnetization, when temperature of the superfluid $^3\text{He-B}$ was stable, we set the magnetic field (B_0) to 2.5 mT, and measured a collection of the resonance curves at various excitations at this field. Thereafter, we reduced the magnetic field B_0 slowly by 0.25 mT and repeated the measurements of the resonance characteristics as a function of excitation. We reproduced this measurement procedure while reducing the magnetic field B_0 down to 0.25 mT.

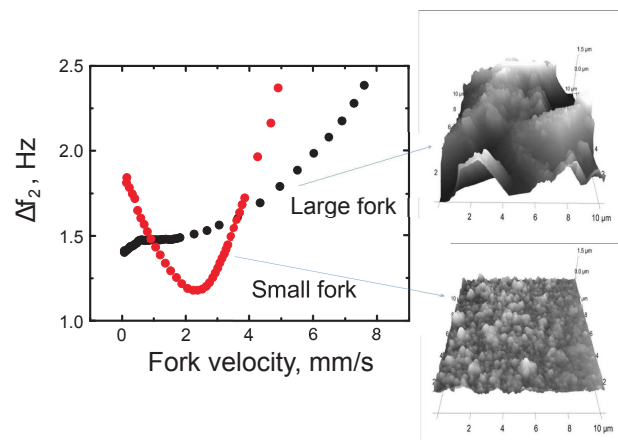


FIG. 2: (Color online) Dependence of the width Δf_2 for large (black) and small (red) tuning forks as a function of fork velocity and images of the surface profiles of tuning forks used in experiment obtained from AFM scans.

EXPERIMENTAL RESULTS AND ANALYSIS

Figure 2 shows the width Δf_2 as a function of the fork velocity measured for the large and small tuning forks in superfluid $^3\text{He-B}$ at temperature of $175\mu\text{K}$ and pressure of 0.1 bar. As one can see, there is a remarkable difference between them. The small tuning fork clearly demonstrates Andreev reflection process [21–23]: as the fork velocity is rising more and more volume excitations undergo the process of Andreev reflection. During this scattering process they exchange a tiny momentum with the fork of the order of $(\Delta/E_F)p_F$, where E_F and p_F are the Fermi energy and the Fermi momentum, respectively. As a result, the fork damping decreases until a critical velocity is reached. At this velocity the fork begins to break the Cooper pairs and its damping rises again. However, this dependence for the large tuning fork is opposite: the process of the Andreev reflection is suppressed, and the damping of the large fork increases with its velocity at

the beginning. Different the width Δf_2 - velocity dependence for the large fork presented in Fig. 2 suggests a presence of some processes leading to the suppression of the Andreev reflection and/or another dissipation mechanism than the Andreev reflection.

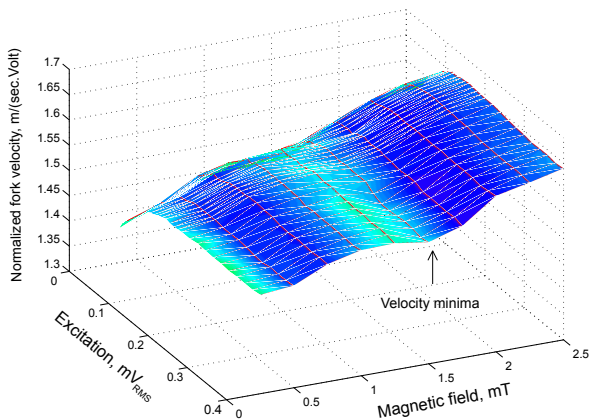


FIG. 3: (Color online) Dependence of the normalized tuning fork velocity (fork velocity over excitation voltage) as a function of the fork velocity and applied magnetic field B_0 . Dependence clearly shows a presence of the velocity minima at magnetic fields that satisfy the Larmor resonance condition $\omega_L = \gamma(B_0 + B_{rem})$.

We assume that at temperature $\sim 175\mu\text{K}$, the density of excitations near the surface of both forks satisfies the condition $\phi_S > \phi_V$. However, we suppose that “non-standard” behavior of the large tuning fork is caused by the different quality of its surface compared with that of the small fork. While the surface of the large fork is corrugated, the surface of the small fork is much smoother (see Fig. 2). Fork motion in superfluid $^3\text{He-B}$ is associated with creation of the back-flow i.e. the flow of the superfluid component around tuning fork’s body on the scale of the slip length [24, 25]. The back-flow shifts the energy of excitations by $\mathbf{p}_F \cdot \mathbf{v}$, where \mathbf{v} is the fork velocity. As a consequence, the excitations having energy less than $\Delta + \mathbf{p}_F \cdot \mathbf{v}$ are scattered via Andreev process. This simple model assumes that direction of the back-flow is correlated with the direction of the fork velocity i.e. the back-flow flows in opposite direction to the tuning fork motion. However, assuming that the scale of the surface roughness of the large fork is larger than the slip length (see Fig. 2), the oscillating surface of the large fork makes the back-flow random. That is, the flow is not correlated with direction of the tuning fork motion. This means that there are excitations reflected via Andreev process there due to the back-flow flowing in different directions to that of the tuning fork velocity. Such reflected excitations are practically “invisible” to the fork. On the other hand, the small fork is sensitive to the Andreev reflection

supposing that the scale of its surface roughness is less or comparable to the slip length. We presume that above presented mechanism stays behind the suppression of the Andreev reflection in case of the large fork. However, to confirm this hypothesis additional work has to be done. Regarding to the rise of the large fork damping at low velocities, the origin of this phenomenon is unclear yet, and it is not a subject of this article.

Another unexpected results were observed while measuring the damping of the large tuning fork motion in superfluid $^3\text{He-B}$ at temperature of $175\mu\text{K}$ in magnetic field. We surprisingly found that the damping of the large fork motion is magnetic field dependent and shows a maximum.

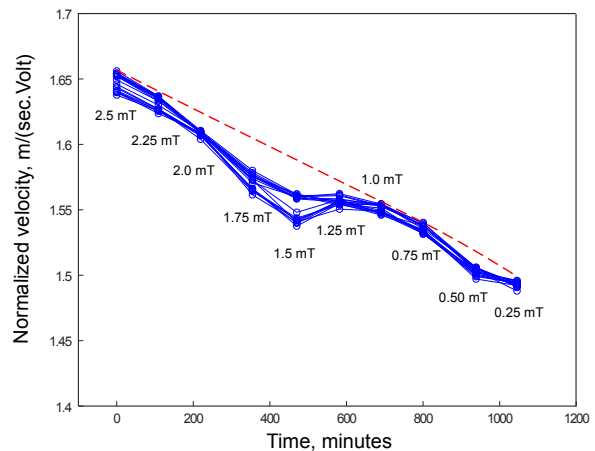


FIG. 4: (Color online) Time dependencies of the normalized tuning fork velocity (fork velocity over excitation voltage) measured at different magnetic fields as showed. The points represent the data measured for various excitations at particular field. Figure clearly shows a presence of the velocity minima at magnetic field corresponding to the Larmor resonance condition $\omega_L = \gamma(B_0 + B_{rem})$. The dashed line illustrates a small thermal background caused by a parasitic heat leak.

Figure 3 shows the results of above mentioned measurements in a form of the dependence of the normalized tuning fork velocity as a function of the fork velocity and magnetic field. This dependence clearly shows a presence of the minima in the fork velocity at the same value of the magnetic field. Presented dependencies are masked by a tiny thermal background due to a small warm-up caused by a parasitic heat leak into nuclear stage (see Fig. 4). Time evolution of the thermal background was modeled using the polynomial dependence $a \cdot t^2 + b \cdot t + c$, where a, b, c are fitting parameters and t is the time. We determined these parameters for particular excitation by fitting the time dependence via points measured at 2.5, 2.25, 1.0, 0.75 and 0.25 mT (see illustrative the red dashed line in Fig. 4). When we subtracted-off the

thermal background, the resulting dependencies are presented in Fig. 5. Figure 5 shows two dependencies of the tuning fork velocity as a function of excitation and magnetic field B_0 . These two dependencies measured during two subsequent demagnetizations demonstrate their reproducibility.

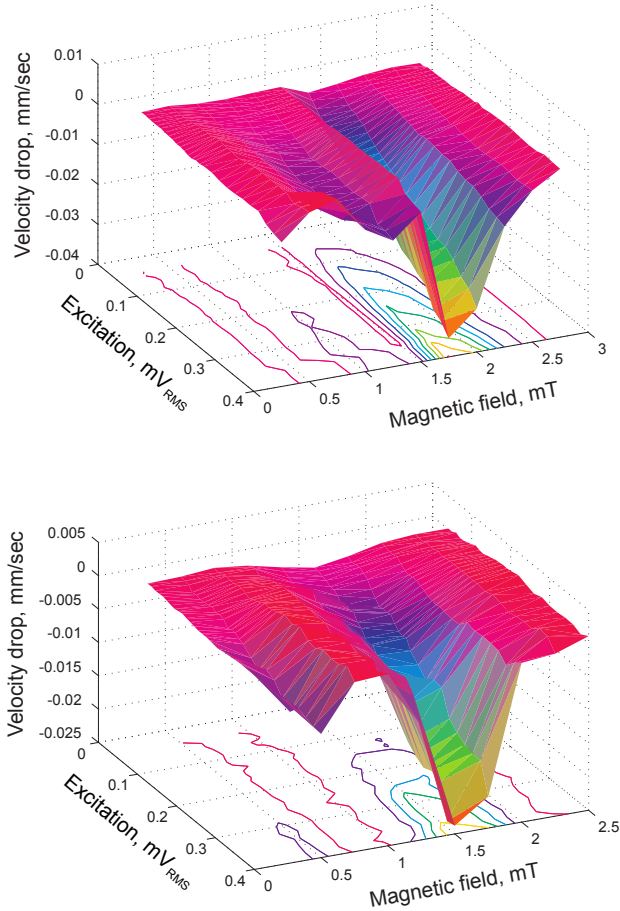


FIG. 5: (Color online) Two dependencies of the velocity drop of the tuning fork expressed as a function of the magnetic field B_0 and excitation voltage measured during two subsequent demagnetizations. Both dependencies show a clear minimum in velocity as function of the magnetic field at value that corresponds to the Larmor resonance frequency $\omega_F = \gamma(B_0 + B_{rem})$. We note that value of B_{rem} is ~ -0.5 mT.

Figure 5 manifests a new and intriguing phenomenon: a presence of the velocity minima (i.e. an additional damping) at magnetic fields which satisfy the Larmor resonance condition $\omega = \gamma(B_0 + B_{rem}) = \gamma B$, where ω is the angular frequency of the tuning fork ($\omega \simeq 2\pi \cdot 32.4$ kHz), γ is the ^3He gyromagnetic ratio ($\gamma = -2\pi \cdot 32.4 \times 10^3$ rad/s.mT), B_0 and B_{rem} is the magnetic field applied and remnant magnetic field from demagnetization magnet, respectively. We interpret this phenomenon as an effect of NMR on the anisotropic magnetic moment

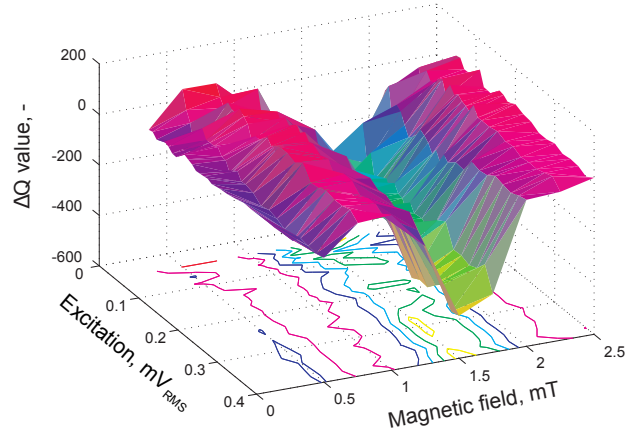


FIG. 6: (Color online) Dependence of the tuning fork Q-values as a function of magnetic field B_0 and excitation voltage. The deep minimum corresponds to nuclear magnetic resonance of the magnetic layer formed on tuning fork surface.

\mathbf{M} formed on the horizontal surface of the tuning fork. Formation of the anisotropic magnetic moment \mathbf{M} is a consequence of the symmetry violation of the $^3\text{He-B}$ order parameter by the fork surface, simultaneously modifying the excitation spectrum. At zero temperature limit, where measurements were performed, the influence of the surface states dominates, as the rest of superfluid $^3\text{He-B}$ in volume behaves like a vacuum. Figure 6 shows the same NMR effect, however, as a drop of the tuning fork Q-value in dependence on the excitation and magnetic field.

In order to explain the measured dependencies we propose a simple phenomenological model as follows. The fork's motion in zero magnetic field can be described by the equation

$$\frac{d^2\alpha}{dt^2} + \Gamma \frac{d\alpha}{dt} + \omega_0\alpha = F_m \sin(\omega t), \quad (1)$$

where Γ is the damping coefficient characterizing the fork's interaction with surrounding superfluid $^3\text{He-B}$, ω_0 is the fork resonance frequency in vacuum, ω is the angular frequency of the external force, α is the deflection angle of the tuning fork arm from equilibrium and F_m is the force amplitude normalized by the mass m and by the length l of the tuning fork arm. We assume that fork's deflections are small enough and therefore interaction of the tuning fork with superfluid $^3\text{He-B}$ acts in linear regime i.e. we neglect processes of the Andreev reflection [21, 23].

By applying external magnetic field $\mathbf{B} = (0, 0, B_0 + B_{rem}) = (0, 0, B)$, the magnetic moment \mathbf{M}_0 is formed on the fork's horizontal surfaces. The magnetic moment \mathbf{M}_0 of the surface layer includes the strong spin anisotropy of the superfluid ^3He layer together with mag-

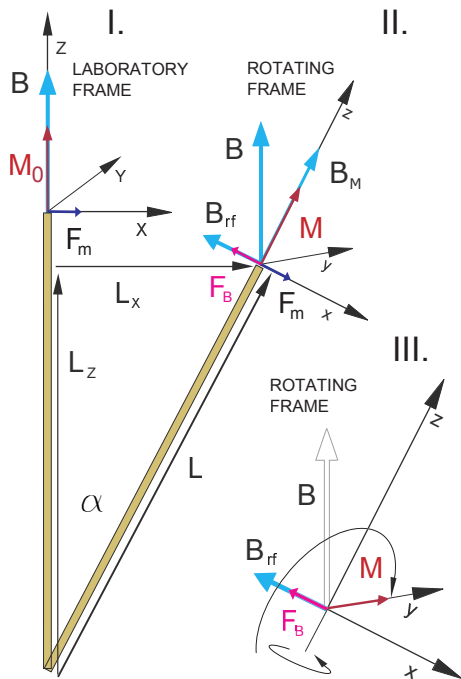


FIG. 7: (Color online) Schematic view on individual vectors for two positions of the tuning fork. In stationary position (I.) Zeeman energy is minimized and magnetic torque is zero. When fork is deflected by external force \mathbf{F}_m (II.), the rise of Zeeman energy due to anisotropy of the magnetic moment \mathbf{M} is associated with emergence of the force \mathbf{F}_B which acts against external force \mathbf{F}_m and causes additional, magnetic field dependent damping. When NMR condition is satisfied (III.) i.e. when $B_{eff} = B_{rf}$, magnetic moment \mathbf{M} precesses in $z - y$ plane around B_{rf} in rotating frame of the reference.

netic moments of solid ^3He atoms covering the fork's surface [5, 26, 33, 34]. However, based on measurements presented in [26], we presume that magnetic moments of solid ^3He atoms behave as a paramagnet and, on a time scale of the fork oscillation period, its Zeeman energy is always minimized. Therefore, magnetic property of the surface layer of superfluid $^3\text{He-B}$ is responsible for the anisotropy of the magnetic moment \mathbf{M} . According to [5], the anisotropic spin susceptibility of the surface layer of superfluid $^3\text{He-B}$ at $T \rightarrow 0$ can be expressed as

$$\chi_{zz} = \frac{\hbar^2 \gamma^2 k_F^2}{16\pi\Delta}, \quad (2)$$

where $p_F = \hbar k_F$. This susceptibility is as large as the normal state susceptibility χ_N multiplied by the width $1/\kappa = \hbar v_F/\Delta$ of the bound states. Here, v_F is the Fermi velocity.

In general, due to surface diffusivity the orientation of \mathbf{M}_0 can be tilted from the field direction \mathbf{B} . However, we shall assume for simplicity that $\mathbf{M}_0 = (0, 0, M_0)$. When fork oscillates in external magnetic field \mathbf{B} , the normal to its horizontal surface \mathbf{m} is deflected from the direction of the external magnetic field \mathbf{B} (see Fig. 7). This

means that anisotropic magnetic moment \mathbf{M} of the surface layer undergoes the same deflections (oscillations). We assume that during fork oscillations the magnetic moment of solid ^3He layer follows the direction of magnetic field \mathbf{B} minimizing its Zeeman energy. Therefore, in the reference frame connected to the anisotropic magnetic moment \mathbf{M} , this moment \mathbf{M} experiences a linearly polarized alternating magnetic field \mathbf{B}_{rf} of amplitude $B_{rf} = B \sin(\alpha) \simeq B\alpha$ oscillating with angular frequency ω of the tuning fork. While magnetic field magnitude in the direction of magnetic moment \mathbf{M} is $B_M = B \cos(\alpha) \simeq B$. Thus, a typical experimental NMR configuration is set up. However, here the “virtual” excitation rf-field \mathbf{B}_{rf} acting on anisotropic magnetic moment \mathbf{M} is generated by harmonic mechanical motion of the tuning fork. We suppose that magnetic torque $\mathbf{M} \times \mathbf{B}$ acting on the anisotropic magnetic moment \mathbf{M} is equivalent to the mechanical torque $\mathbf{L} \times \mathbf{F}_B$, where $\mathbf{L} = (L_x, 0, L_z)$ is the vector pointed in direction of \mathbf{M} having the magnitude equal to the length of the oscillating fork prong l . The force \mathbf{F}_B emerges from the rising of the Zeeman energy $(-\mathbf{M} \cdot \mathbf{B})$ due to deflection of \mathbf{M} from the field direction, acts against excitation force \mathbf{F}_m and causes additional field-dependent damping of the tuning fork motion. This force can be expressed as

$$\mathbf{F}_B = \frac{1}{\gamma l^2} \frac{d\mathbf{M}}{dt} \times \mathbf{L}. \quad (3)$$

In order to obtain time dependence of \mathbf{F}_B one has to determine dynamics of the magnetic moment \mathbf{M} which is governed by the Bloch's equation (in rotating reference frame)

$$\frac{\delta\mathbf{M}}{\delta t} = \gamma(\mathbf{M} \times \mathbf{B}_{eff}) + \frac{\mathbf{M}_0 - \mathbf{M}}{T_i}. \quad (4)$$

Here $\mathbf{M} = (M_x, M_y, M_z)$, $\mathbf{B}_{eff} = (-B_{rf}, 0, B - \omega/\gamma)$, and the second term on the right side describes the processes of the energy dissipation being characterized by the relaxation time constants T_i with $i = 1$ for z -component and $i = 2$ for xy -component of the magnetic moment \mathbf{M} . Assuming that magnetic relaxation processes act solely in the magnetic layer near fork surface and using the geometry of the problem, the amplitude of the force F_B acting against excitation force F_m can be expressed as

$$F_B = \frac{1}{\gamma l} \frac{dM_y}{dt} = \frac{1}{\gamma l} [\chi_D \cos(\omega t) + \chi_A \sin(\omega t)] B \frac{d\alpha}{dt}, \quad (5)$$

where M_y is the y -component of magnetic moment \mathbf{M} in the laboratory frame, ω is the tuning fork angular frequency, χ_A denotes the absorption component of the magnetic susceptibility of the layer expressed in the form

$$\chi_A = \frac{\chi_L \omega_B T_2}{1 + (\omega_B - \omega)^2 T_2^2} \quad (6)$$

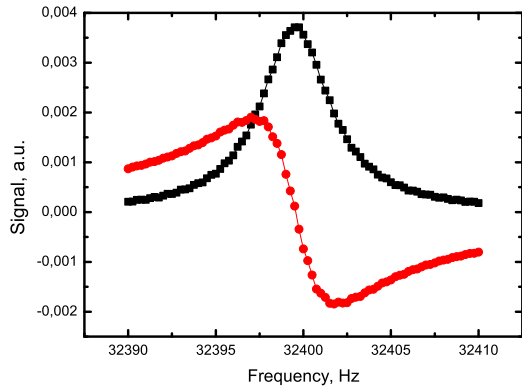


FIG. 8: (Color online) Example of the calculated resonance characteristics of the tuning fork using equation (8) for magnetic field 2.25 mT and excitation 175 mV.

and χ_D denotes the dispersion component in the form

$$\chi_D = \frac{\chi_L \omega_B (\omega_B - \omega) T_2^2}{1 + (\omega_B - \omega)^2 T_2^2}. \quad (7)$$

Here $\omega_B = \gamma B$ and $M = \chi_L B$, where χ_L stands for the magnetic susceptibility of the ^3He -layer. Adding the term (5) into equation (1), one gets nonlinear differential equation describing the tuning fork motion with anisotropic magnetic layer on its horizontal surface in external magnetic field in form

$$\frac{d^2\alpha}{dt^2} + \Gamma \frac{d\alpha}{dt} + \frac{1}{\gamma l^2 m} \frac{dM_Y}{dt} + \omega_0 \alpha = F_m \sin(\omega t). \quad (8)$$

Applying Runge-Kutta method we numerically calculated the time evolution of the tuning fork response described by the equation (8) as a function of applied external force (in frequency and amplitude) and magnetic field. Calculations took into account transient phenomena. Reaching a steady state of the fork motion, the calculated values were multiplied by the "reference" signals simulating excitations with aim to obtain the resonance characteristics i.e. the absorption and the dispersion component. The magnetic properties of surface layer were characterized by the spin-spin relaxation time constant $T_2 = 28 \mu\text{sec}$. Figure 8 shows an example of the tuning fork response calculated by using equation (8) in form of the resonance characteristics. Calculated resonance characteristics were fitted by means of the Lorentz function in order to obtain experimentally measurable parameters: the velocity amplitude, the width and the resonance frequency as the function of the excitation and magnetic field. Figure 9 summarizes theoretically calculated dependence of the tuning fork velocity drop as a function of driving force (excitation voltage) and magnetic field. Presented dependencies confirm the presence

of the velocity minima at magnetic field corresponding to the Larmor resonance condition for ^3He and they are in very good qualitative agreement with those obtained experimentally (see Fig. 5).

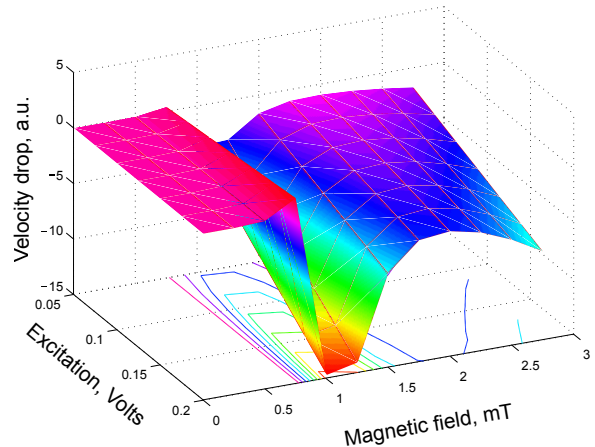


FIG. 9: (Color online) Theoretical dependence of the tuning fork velocity drop as a function of the magnetic field B_0 and excitation voltage calculated using equation (8).

DISCUSSION

Although, we have presented a simple theoretical model using a phenomenological approach, we obtained reasonable qualitative agreement with experiment. However, it is worth to say that there is a set of theoretical papers dealing with problem of the Andreev-Majorana surface states in topological superfluid $^3\text{He-B}$ on the level of the order parameter [5, 27–34]. In light of this, let us discuss our experimental results and compare them with theoretical models.

In particular, the spin dynamics and an effect of NMR on the magnetic moment of the surface states had recently been theoretically investigated by M. A. Silaev [34]. Using assumptions of a flat surface, i.e. that the vector \mathbf{n} representing a rotation axis of the superfluid $^3\text{He-B}$ order parameter is parallel to magnetic field \mathbf{B}_0 , he showed that standard transverse NMR technique does not allow to excite the magnetic moment of the surface states at Larmor frequency due to two reasons. The first, a mini-gap presented at the surface state spectrum has a broader energy gap E_g than corresponding Larmor frequency due to Fermi-liquid corrections ($E_g \sim 4\hbar\omega_L$). The second, the probability of the NMR excitation in surface states spectrum is proportional to the deflection angle β_n of the vector \mathbf{n} from the spin quantization axis defined by magnetic field \mathbf{B}_0 . For a flat surface, the angle β_n is rather small leading to a strong suppression of the NMR response from the surface states. However, in

order to excite the Andreev-Majorana surface states using a transverse NMR technique, the vector \mathbf{n} has to be deflected from magnetic field direction by an angle β_n , so that the effective driving field \mathbf{B}_{eff} has a component parallel to the spin quantization axis [34].

The Lancaster group [35] performed the NMR measurements using superfluid $^3\text{He-B}$ near a surface in experimental configuration, which is similar to that as assumed in [34]. The experimental cell was made from sapphire. However, instead of a flat horizontal surface, their cell had a semi-spherical end cap. Pulsed NMR technique allowed them to create a long lived state with coherent spin precession named as persistently precessing domain (PPD) [36, 37]. Using magnetic field gradient they were able to control the position of the PPD with respect to the horizontal wall of the cell [38]. They showed that the closer the Larmor resonance condition is to the cell horizontal surface, the shorter the PPD signal life time is. The presence of the cell surface reduces the signal life time by four orders of magnitude [35]. In the light of theory [34], the interpretation of this phenomena needs to be elucidated.

Our experimental configuration of the NMR detection using mechanical resonator is completely different from that of a standard transverse NMR technique. The most important difference is that we did not apply any external rf-field $\mathbf{B}_{r,f}$ to excite magnetic moments in superfluid $^3\text{He-B}$. The only magnetic field presented is the static magnetic field \mathbf{B} . An excitation rf-field $\mathbf{B}_{r,f}$ is a “virtual” field, which is experienced only by the anisotropic magnetic moment \mathbf{M} during fork oscillations.

Harmonic oscillations of the tuning fork arms lead to the oscillation of the whole texture of \mathbf{n} vectors causing their time dependent deflection from the quantized axis defined by the constant magnetic field \mathbf{B} . The amplitude of the tuning fork oscillation at maximum excitation was ~ 2 nm. This is much less than the coherence length and the size of surface roughness. Low oscillation amplitude also reduces the bulk effects. Diffusivity of the tuning fork surface (see Fig. 2) ensures the deflections of the \mathbf{n} vectors in a broad spectrum of angles β_n from the field direction. This is a configuration, which according to model [34], satisfies the condition for the observation of transverse NMR of the surface states in superfluid $^3\text{He-B}$. However, according to our opinion, the assumptions of the theoretical model [34] do not fully correspond to the conditions of the experiment presented here and the model itself could be extended for them.

On the other hand, theoretical model presented in [5] suggests that strong spin anisotropy of superfluid ^3He layer near the surface is large enough to be observed experimentally. We think that above mentioned experimental technique using mechanical resonators (e.g. tuning forks) with various surface roughness and resonance frequencies is a way. However, the open question is an influence of the solid ^3He on this phenomenon. Although

we assumed a paramagnetic property of the solid ^3He layer, the magnetic susceptibility of the solid ^3He dominates at ultra low temperatures [26]. An influence of solid ^3He could be tested by using ^4He as a coverage on the surface of the tuning fork, since ^4He atoms remove ^3He atoms from the surface. However, ^4He simultaneously covers the heat exchangers inside nuclear stage and this reduces the cooling efficiency of the ^3He liquid. As the measurements are performed in temperature range below $200 \mu\text{K}$, the test of influence of the ^3He solid layer on the observed phenomenon is going to be an experimental challenge.

CONCLUSION

In conclusion, we have observed the NMR effect on anisotropic magnetic moment of the superfluid surface layer, including Andreev-Majorana fermionic excitation formed on the resonators’ surface, being detected as additional magnetic field dependent damping of its mechanical motion. Further work is required to develop this technique, which in combination with e.g. acoustic method [7], or non-standard NMR technique based on PPD [35], or thermodynamic method [39] opens a possibility to study the spin dynamics of excitations trapped in SABS in topological superfluid $^3\text{He-B}$ and, perhaps to prove their Majorana character experimentally. Finally, a development of a theory considering oscillations of \mathbf{n} vectors representing the order parameter of superfluid ^3He near a surface at constant magnetic field, i.e. a theory for the condition of presented experiment would be very useful and challenging.

ACKNOWLEDGMENTS

We acknowledge the support of APVV-14-0605, VEGA 2/0157/14, Extrem II - ITMS 26220120047 and European Microkelvin Platform, H2020 project 824109. We wish to thank to M. Kupka for fruitful discussion, V. Komanický for AFM scans of tuning forks, and to Š. Bicák and G. Pristáš for technical support. Support provided by the U.S. Steel Košice s.r.o. is also very appreciated.

* Electronic Address: skyba@saske.sk

- [1] G. E. Volovik, *Universe in Helium-3 Droplet*, Clarendon Press, Oxford (2003).
- [2] W. J. Gully, D. D. Osheroff, D. T. Lawson, R. C. Richardson, and D. M. Lee, *Phys. Rev. A* **8**, 1633 (1973).
- [3] V. V. Dmitriev, A. A. Senin, A. A. Soldatov, and A. N. Yudin, *Phys. Rev. Lett.* **115**, 165304 (2015).

- [4] N. Zhelev, M. Reichel, T. S. Abhilash, E. N. Smith, K. X. Nguyen, E. J. Mueller, and J. M. Parpia, *Nature Comm.* **7**, 12975 (2016).
- [5] Y. Nagato, S. Higashitani, K. Nagai, *J. of the Phys. Soc. of Japan* **78** 123603 (2009).
- [6] Suk Bum Chung, Shou-Cheng Zhang, *Phys. Rev. Lett.* **103**, 235301 (2009).
- [7] S. Murakawa, Y. Tamura, Y. Wada, M. Wasai, M. Saitoh, Y. Aoki, R. Nomura, Y. Okuda, Y. Nagato, M. Yamamoto, S. Higashitani, and K. Naga, *Phys. Rev. Lett.* **103**, 155301 (2009).
- [8] G. E. Volovik, *JETP Lett.* **91**, 201 (2010).
- [9] T. Mizushima, K. Machida, *J. Low Temp. Phys.* **162** 204 (2011).
- [10] Y. Nagato, M. Yamamoto, K. Nagai, *J. Low Temp. Phys.* **110**, 1135 (1998).
- [11] A. B. Vorontsov, J. A. Sauls, *Phys. Rev. B* **68**, 064508 (2003).
- [12] Y. Aoki, Y. Wada, M. Saitoh, R. Nomura, Y. Okuda, Y. Nagato, M. Yamamoto, S. Higashitani, and K. Nagai, *Phys. Rev. Lett.* **95**, 075301 (2005).
- [13] D. I. Bradley, P. Crookston, S. N. Fisher, A. Ganshin, A. M. Guénault, R. P. Haley, M. J. Jackson, G. R. Pickett, R. Schanen, V. Tsepelin, *J. Low Temp. Phys.* **157**, 476 (2009).
- [14] D. I. Bradley, S. N. Fisher, A. M. Guénault, R. P. Haley, R. C. Lawson, G. R. Pickett, R. Schanen, M. Skyba, V. Tsepelin, and D. E. Zmeev, *Nature Physics*, **12**, 1017 (2016).
- [15] P. Zheng, W. G. Jiang, C. S. Barquist, Y. Lee, and H. B. Chan, *Phys. Rev. Lett.* **117**, 195301 (2016).
- [16] P. Zheng, W. G. Jiang, C. S. Barquist, Y. Lee, and H. B. Chan, *Phys. Rev. Lett.* **118**, 065301 (2017).
- [17] R. Blaauwgeers, M. Blažková, M. Človečko, V. B. Eltsov, R. de Graaf, J. Hosio, M. Krusius, D. Schmoranzler, W. Schoepe, L. Skrbek, P. Skyba, R. E. Solntsev, D. E. Zmeev, *J. Low Temp. Phys.* **146**, 537 (2007).
- [18] P. Skyba, *J. Low Temp. Phys.* **160**, 219 (2010).
- [19] S. Holt, P. Skyba, *Rev. Sci. Instrum.* **83**, 064703 (2012).
- [20] P. Skyba, J. Nyéki, E. Gažo, V. Makróczyová, Yu. M. Bunkov, D. A. Sergackov, A. Feher, *Cryogenics* **37**, 293 (1997).
- [21] S. N. Fisher, A. M. Guénault, C. J. Kennedy, G. R. Pickett, *Phys. Rev. Lett.* **63**, 2566 (1989).
- [22] D. I. Bradley, M. Človečko, E. Gažo, P. Skyba, *J. Low Temp. Phys.* **152**, 147 (2008).
- [23] M. Človečko, E. Gažo, M. Kupka, M. Skyba, P. Skyba, *J. Low Temp. Phys.* **162** 669 (2011).
- [24] D. Einzel, H. Højgaard, Jensen, H. Smith, P. Wölfle, *J. Low Temp. Phys.* **53**, 695 (1983).
- [25] D. Einzel, P. Wölfle, H. Højgaard Jensen, H. Smith, *Phys. Rev. Lett.* **52**, 1705 (1984).
- [26] D. I. Bradley, S. N. Fisher, A. M. Guénault, R. P. Haley, N. Mulders, G. R. Pickett, D. Potts, P. Skyba, J. Smith, V. Tsepelin, and R. C. V. Whitehead, *Phys. Rev. Lett.* **105**, 125303 (2010).
- [27] G. E. Volovik, *JETP Lett.* **90**, 440 (2009).
- [28] M. A. Silaev, *Phys. Rev. B* **84**, 144508 (2011).
- [29] J. A. Sauls, *Phys. Rev. B* **84**, 214509 (2011).
- [30] Y. Tsutsumi, M. Ichioka, and K. Machida, *Phys. Rev. B* **83**, 094510 (2011).
- [31] T. Mizushima, M. Sato and K. Machida, *Phys. Rev. Lett.* **109**, 165301 (2012).
- [32] T. Mizushima, Y. Tsutsumi, M. Sato, and K. Machida, *J. Phys.: Condens. Matter* **27**, 113203 (2015).
- [33] M. A. Silaev, G. E. Volovik, *JETP* **119**, 1042 (2014).
- [34] M. A. Silaev, *J. Low Temp. Phys.* **191**, 393 (2018).
- [35] S. N. Fisher, G. R. Pickett, P. Skyba, and N. Suramlishvili, *Phys. Rev. B* **86**, 024506 (2012).
- [36] Yu. M. Bunkov, S. N. Fisher, A. M. Guénault, G. R. Pickett, *Phys. Rev. Lett.* **69**, 3092 (1992).
- [37] M. Kupka, P. Skyba, *Physics Letters A* **317**, 324 (2003).
- [38] D. I. Bradley, D. O. Clubb, S. N. Fisher, A. M. Guénault, C. J. Matthews, G. R. Pickett, P. Skyba, *J. Low Temp. Phys.* **134** 351 (2004).
- [39] Yu. M. Bunkov, *J. Low Temp. Phys.* **175**, 385 (2014).